World Academy of Science, Engineering and Technology
International Journal of Mechanical and Mechatronics Engineering
Vol:4, No:3, 2010

Internal Loading Distribution in Statically Loaded Ball Bearings Subjected to a Centric Thrust Load: Numerical Aspects

Mário C. Ricci

***Abstract*—**A known iterative computational procedure is used for internal normal ball loads calculation in statically loaded single-row, angular-contact ball bearings, subjected to a known thrust load, which is applied in the inner ring at the geometric bearing center line. Numerical aspects of the iterative procedure are discussed. Numerical examples results for a 218 angular-contact ball bearing have been compared with those from the literature. Twenty figures are presented showing the geometrical features, the behavior of the convergence variables and the following parameters as functions of the thrust load: normal ball loads, contact angle, distance between curvature centers, and normal ball and axial deflections between the raceways.

***Keywords*—**Ball, Bearing, Static, Load, Iterative, Numerical, Method.

I. Introduction

BALL and roller bearings, generically called *rolling bearings*, are commonly used machine elements. They are employed to permit rotary motions of, or about, shafts in simple commercial devices such as bicycles, roller skates, and electric motors. They are also used in complex engineering mechanisms such as aircraft gas turbines, rolling mils, dental drills, gyroscopes, and power transmissions.

The standardized forms of ball or roller bearings permit rotary motion between two machine elements and always include a complement of ball or rollers that maintain the shaft and a usually stationary supporting structure, frequently called a *housing*, in a radially or axially spaced-apart relationship. Usually, a bearing may be obtained as a unit, which includes two steel rings each of which has a hardened raceway on which hardened balls or rollers roll. The balls or rollers, also called *rolling elements*, are usually held in an angularly spaced relationship by a *cage*, also called a *separator* or *retainer*.

There are many different kinds of rolling bearings. This work is concerned with *single-row angular-contact ball bearings* (Fig. 1) that are designed to support combined radial and thrust loads or heavy thrust loads depending on the *contact angle* magnitude. The bearings having large contact angle can support heavier thrust loads. Fig. 1 shows bearings having small and large contact angles. The bearings generally have groove curvature radii in the range of 52-53% of the ball diameter. The contact angle does not usually exceed 40°.

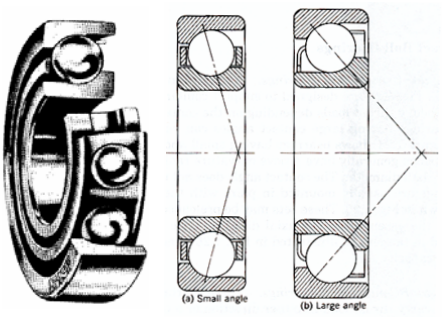

Fig. 1 Angular-contact ball bearing

This work is devoted to study of the internal loading distribution in statically loaded ball bearings. Several researchers have studied the subject as, for example, Stribeck [1], Sjoväll [2], Jones [3] and Rumbarger [4]. The methods developed by them to calculate distribution of load among the balls and rollers of rolling bearings can be used in most bearing applications because rotational speeds are usually slow to moderate. Under these speed conditions, the effects of rolling element centrifugal forces and gyroscopic moments are negligible. At high speeds of rotation these body forces become significant, tending to alter contact angles and clearance. Thus, they can affect the static load distribution to a great extension.

Harris [5] described methods for internal loading distribution in statically loaded bearings addressing pure radial; pure thrust (centric and eccentric loads); combined radial and thrust load, which uses radial and thrust integrals introduced by Sjoväll; and for ball bearings under combined radial, thrust, and moment load, initially due to Jones.

There are many works describing the parameters variation models under static loads but few demonstrate such variations in practice, even under simple static loadings. The author believes that the lack of practical examples is mainly due to the inherent difficulties of the numerical procedures that, in general, deal with the resolution of several non-linear

M. C. Ricci is with the Brazilian Institute for Space Research, São José dos Campos, 12227-010 Brazil (e-mail: mariocesarricci@uol.com.br).

M. C. Ricci thanks the financial support provided by the Brazilian Institute for Space Research (INPE), the Brazilian Scientific and Technological Development Council (CNPq), and The State of São Paulo Research (FAPESP).

algebraic equations, which must to be solved simultaneously.

In an attempt to cover this gap studies are being developed in parallel [6]-[12]. Particularly, in this work a known iterative computational procedure (see [5], p. 245) is used to obtain internal normal ball loads in statically loaded single-row, angular-contact ball bearings, subjected to a known thrust load, which is applied in the inner ring at the geometric bearing center line. Although the method is well known, aspects of the numerical procedure and the behavior of the variables under convergence haven't been sufficiently explored in the literature. So, numerical aspects of the iterative procedure are discussed and numerical examples results for a 218 angular-contact ball bearing have been compared with those from the literature. Twenty figures are presented showing the geometrical features, the behavior of convergence variables and the following parameters as functions of the external thrust load: normal ball loads, contact angle, distance between curvature centers, and normal ball and axial deflections.

II. Symbols

a	Semimajor axis of the projected contact, m
A	Distance between raceway groove curvature centers at unloaded position, m
b	Semiminor axis of the projected contact, m
B	$f_o + f_i - 1$, Total curvature
d	Raceway diameter, m
d_a	Bearing outer diameter, m
d_b	Bearing inner diameter, m
d_e	Bearing pitch diameter, m
D	Ball diameter, m
E	Modulus of elasticity, N/m^2
E'	Effective elastic modulus, N/m^2
$\mathbf{E}$	Elliptic integral of second kind
f, f_s	Raceway groove radius ÷ D; shock factor
F	Applied load, N
k	a/b
K	Load-deflection factor, N/m$^{3/2}$
$\mathbf{K}$	Elliptic integral of first kind
P_d	Diametral clearance, m
P_e	Free endplay, m
Q	Ball-raceway normal load, N
r	Raceway groove curvature radius; solids curvature radius, m
s	Distance between loci of inner and outer raceway groove curvature centers, m
R	Curvature radius, m
Z	Number of rolling elements
β, β', β''	Contact angle, rad, ^{o}
β_f	Free contact angle, rad, ^{o}
γ	$D \cos \beta / d_e$
Γ	Curvature difference
δ	Deflection or contact deformation, m
$\Delta\psi$	Angular spacing between rolling elements, rad,^{o}
υ	Poisson's ratio
φ	Auxiliary angle
ψ	Azimuth angle, rad, ^{o}

Subscripts:

a	Refers to solid a or axial direction
b	Refers to solid b
x,y	Refers to coordinate system
i	Refers to inner raceway
j	Refers to rolling element position
n	Refers to direction collinear with normal load
o	Refers to outer raceway

III. Geometry Of Ball Bearings

In this section, the principal geometrical relationships for an unloaded ball bearing are summarized. The radial cross section of a single-row ball bearing shown in Fig. 2 depicts the *diametral clearance* and various diameters. The *pitch diameter*, d_e, is the mean of the inner- and outer-race diameters, d_i and d_o, respectively, and is given by

$$d_e = \frac{1}{2}(d_i + d_o). \tag{1}$$

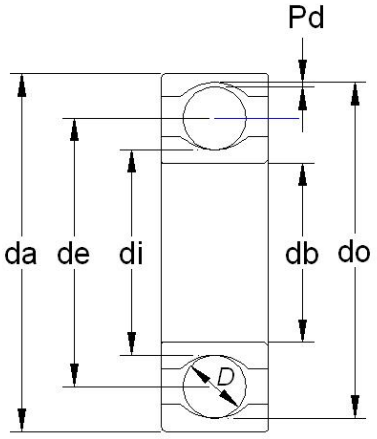

Fig. 2 Radial cross section of a single-row ball bearing

The diametral clearance, P_d, can be written as

$$P_d = d_o - d_i - 2D. \tag{2}$$

Race conformity is a measure of the geometrical conformity of the race and the ball in a plane passing through the bearing axis (also named center line or rotation axis), which is a line passing through the center of the bearing perpendicular to its plane and transverse to the race. Fig. 3 depicts a cross section of a ball bearing showing race conformity, expressed as

$$f = r / D. \tag{3}$$

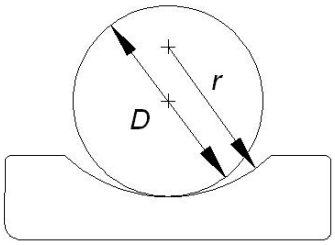

Fig. 3 Cross section of a ball and an outer race showing race conformity

Radial bearings have some axial play since they are generally designed to have a diametral clearance, as shown in Fig. 4(a). Fig. 4(b) shows a radial bearing with contact due to the axial shift of the inner and outer rings when no measurable force is applied. The radial distance between the curvature centers of the two races are the same in the Figs. 4(a) and (b). Denoting quantities referred to the inner and outer races by subscripts *i* and *o*, respectively, this radial distance value can be expressed as $A - P_d/2$, where $A = r_o + r_i - D$ is the curvature centers distance in the shifted position given by Fig. 4(b).

Using (3) we can write A as

$$A = BD, \tag{4}$$

where $B = f_o + f_i - 1$ is known as the *total conformity ratio* and is a measure of the combined conformity of both the outer and inner races to the ball.

The *contact angle*, β, is defined as the angle made by a line, which passes through the curvature centers of both the outer and inner raceways and that lies in a plane passing through the bearing rotation axis, with a plane perpendicular to the bearing axis of rotation. The *free-contact angle*, β_f, (Fig. 4(b)) is the contact angle when the line also passes through the points of contact of the ball and both raceways and no measurable force is applied. From Fig. 4(b), the expression for the free-contact angle can be written as

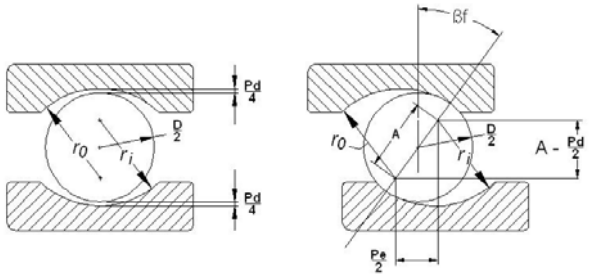

(a) (b)

Fig. 4 Cross section of a radial ball bearing showing ball-race contact due to axial shift of inner and outer rings. (a) Initial position. (b) Shifted position

$$\cos\beta_f = \frac{A - P_d/2}{A}. \tag{5}$$

From (5), the diametral clearance, P_d, can be written as

$$P_d = 2A\left(1 - \cos\beta_f\right). \tag{6}$$

Free endplay, P_e, is the maximum axial movement of the inner race with respect to the outer when both races are coaxially centered and no measurable force is applied. Free endplay depends on total curvature and contact angle, as shown in Fig. 4(b), and can be written as

$$P_e = 2A\sin\beta_f. \tag{7}$$

Considering the geometry of two contacting solids (ellipsoids *a* and *b*) in a ball bearing we can arrive at the two quantities of some importance in the analysis of contact stresses and deformations: The curvature sum, $1/R$, and curvature difference, Γ, which are defined as

$$\frac{1}{R} = \frac{1}{R_x} + \frac{1}{R_y},$$

$$\Gamma = R\left(\frac{1}{R_x} - \frac{1}{R_y}\right),$$

where

$$\frac{1}{R_x} = \frac{1}{r_{ax}} + \frac{1}{r_{bx}},$$

$$\frac{1}{R_y} = \frac{1}{r_{ay}} + \frac{1}{r_{by}},$$

with r_{ax}, r_{bx}, r_{ay} and r_{by}, being the radii of curvature for the ball-race contact.

A cross section of a ball bearing operating at a contact angle β is shown in Fig. 5. Equivalent radii of curvature for both inner- and outer-race contacts in, and normal to, the direction of rolling can be calculated from this figure. Considering *x* the direction of the motion and *y* the transverse direction the radii of curvature for the ball-inner-race contact are

$$r_{ax} = r_{ay} = D/2,$$

$$r_{bx} = \frac{d_e - D\cos\beta}{2\cos\beta},$$

$$r_{by} = -f_i D = -r_i.$$

The radii of curvature for the ball-outer-race contact are

$$r_{ax} = r_{ay} = D/2,$$

$$r_{bx} = -\frac{d_e + D\cos\beta}{2\cos\beta},$$

$$r_{by} = -f_o D = -r_o .$$

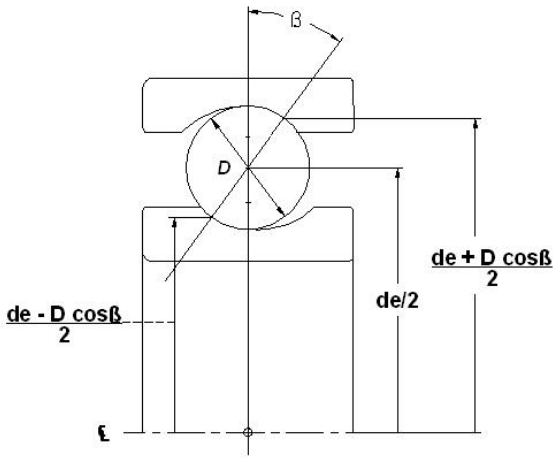

Fig. 5 Cross section of a ball bearing

Let

$$\gamma = \frac{D\cos\beta}{d_e}.$$

Then

$$r_{bx} = \frac{D}{2}\frac{1-\gamma}{\gamma},$$

$$\left.\frac{1}{R}\right|_i = \frac{1}{r_{ax}} + \frac{1}{r_{bx}} + \frac{1}{r_{ay}} + \frac{1}{r_{by}} = \frac{1}{D}\left(4 - \frac{1}{f_i} + \frac{2\gamma}{1-\gamma}\right), \quad (8)$$

$$\Gamma_i = R\left(\frac{1}{r_{ax}} + \frac{1}{r_{bx}} - \frac{1}{r_{ay}} - \frac{1}{r_{by}}\right) = \frac{\frac{1}{f_i} + \frac{2\gamma}{1-\gamma}}{4 - \frac{1}{f_i} + \frac{2\gamma}{1-\gamma}}, \quad (9)$$

for the ball-inner-race contact, and

$$r_{bx} = -\frac{D}{2}\frac{1+\gamma}{\gamma},$$

$$\left.\frac{1}{R}\right|_o = \frac{1}{r_{ax}} + \frac{1}{r_{bx}} + \frac{1}{r_{ay}} + \frac{1}{r_{by}} = \frac{1}{D}\left(4 - \frac{1}{f_o} - \frac{2\gamma}{1+\gamma}\right), \quad (10)$$

$$\Gamma_o = R\left(\frac{1}{r_{ax}} + \frac{1}{r_{bx}} - \frac{1}{r_{ay}} - \frac{1}{r_{by}}\right) = \frac{\frac{1}{f_o} - \frac{2\gamma}{1+\gamma}}{4 - \frac{1}{f_o} - \frac{2\gamma}{1+\gamma}}, \quad (11)$$

for the ball-outer-race contact.

IV. Contact Stress And Deformations

When two elastic solids are brought together under a load, a contact area develops, the shape and size of which depend on the applied load, the elastic properties of the materials, and the curvatures of the surfaces. For two ellipsoids in contact the shape of the contact area is elliptical, with *a* being the semi-major axis in the *y* direction (transverse direction) and *b* being the semi-minor axis in the *x* direction (direction of motion).

The *elliptical eccentricity parameter*, *k*, is defined as

$$k = a/b.$$

From [5], *k* can be written in terms of the curvature difference, Γ, and the *elliptical integrals of the first and second kind*, **K** and **E**, as

$$J(k) = \sqrt{\frac{2\mathbf{K} - \mathbf{E}(1+\Gamma)}{\mathbf{E}(1-\Gamma)}},$$

where

$$\mathbf{K} = \int_0^{\pi/2}\left[1 - \left(1 - \frac{1}{k^2}\right)\sin^2\varphi\right]^{-1/2} d\varphi,$$

$$\mathbf{E} = \int_0^{\pi/2}\left[1 - \left(1 - \frac{1}{k^2}\right)\sin^2\varphi\right]^{1/2} d\varphi.$$

A one-point iteration method, which has been used successfully in the past [13], is used here, where

$$k_{n+1} = J(k_n).$$

When the *ellipticity parameter*, *k*, the *elliptic integrals of the first* and *second kinds*, **K** and **E**, respectively, the normal applied load, *Q*, Poisson's ratio, *v*, and the modulus of elasticity, *E*, of the contacting solids are known, we can write the semi-major and -minor axes of the contact ellipse and the maximum deformation at the center of the contact, from the analysis of Hertz [14], as

$$a = \left(\frac{6k^2\mathbf{E}QR}{\pi E'}\right)^{1/3}, \quad (12)$$

$$b = \left(\frac{6\mathbf{E}QR}{\pi k E'}\right)^{1/3}, \quad (13)$$

$$\delta = \mathbf{K}\left[\frac{9}{2\mathbf{E}R}\left(\frac{Q}{\pi k E'}\right)^2\right]^{1/3}, \quad (14)$$

where

$$E' = \frac{2}{\frac{1-\upsilon_a^2}{E_a} + \frac{1-\upsilon_b^2}{E_b}}.$$

V. Static Load Distribution Under Centric Thrust Load

Methods to calculate distribution of load among the balls and rollers of rolling bearings statically loaded can be found in various papers, [15]. The methods have been limited to, at most, three degrees of freedom in loading and demand the solution of a simultaneous nonlinear system of algebraic equations for higher degrees of freedom. Solution of such equations generally necessitates the use of a digital computer. In certain cases, however – for example, applications with pure radial, pure thrust or radial and thrust loading with nominal clearance – the simplified methods will probably provide sufficiently accurate calculational results.

Having defined a simple analytical expression for the deformation in terms of load in the previous section, it is possible to consider how the bearing load is distributed among the rolling elements. Most rolling-element bearing applications involve steady-state rotation of either the inner or outer race or both; however, the speeds of rotation are usually not so great as to cause ball or roller centrifugal forces or gyroscopic moments of significant magnitudes. In analyzing the loading distribution on the rolling elements, it is usually satisfactory to ignore these effects in most applications. In this section the load deflection relationships for ball bearings are given, along with a specific load distribution consisting of a centric thrust load of statically loaded rolling elements.

A. Load-Deflection Relationships for Ball Bearings

From (14) it can be seen that for a given ball-raceway contact (point loading)

$$Q = K\delta^{3/2}, \tag{15}$$

where

$$K = \pi k E' \sqrt{\frac{2\mathbf{E}R}{9\mathbf{K}^3}}.$$

The total normal approach between two raceways under load separated by a rolling element is the sum of the approaches between the rolling element and each raceway. Hence

$$\delta_n = \delta_i + \delta_o.$$

Therefore,

$$K_n = \left[\frac{1}{1/K_i^{2/3} + 1/K_o^{2/3}}\right]^{3/2}$$

and

$$Q = K_n \delta_n^{3/2}. \tag{16}$$

B. Ball Bearings under Centric Thrust Load

Let a ball bearing with a number of balls, Z, symmetrically distributed about a pitch circle according to Fig. 6, to be subjected to a centric thrust load. Then, a *relative axial displacement*, δ_a, between the inner and outer ring raceways may be expected.

Fig. 7 shows the positions of ball center and raceway groove curvature centers at any angular position ψ, before and after loading, whereas the curvature centers of the raceway grooves are fixed with respect to the corresponding raceway.

From Fig. 7

$$\beta = \cos^{-1}\left(\frac{A - P_d/2}{A + \delta_n}\right) \tag{17}$$

and

$$\delta_a = (A + \delta_n)\sin\beta - A\sin\beta_f. \tag{18}$$

From (5) and (17), the total normal approach between two raceways at any angular position ψ, after the thrust load has been applied, can be written as

$$\delta_n = A\left(\frac{\cos\beta_f}{\cos\beta} - 1\right). \tag{19}$$

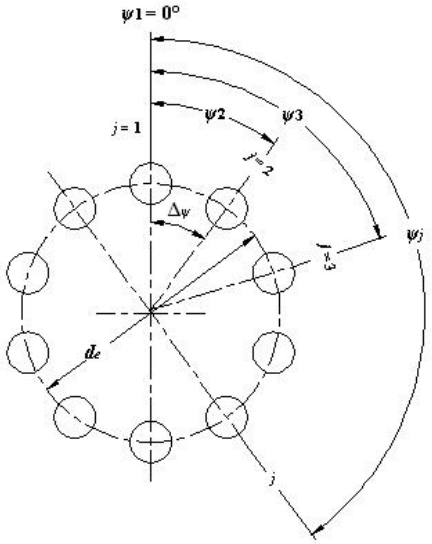

Fig. 6 Ball angular positions in the radial plane that is perpendicular to the bearing's axis of rotation, $\Delta\psi = 2\pi/Z$, $\psi_j = 2\pi/Z(j-1)$

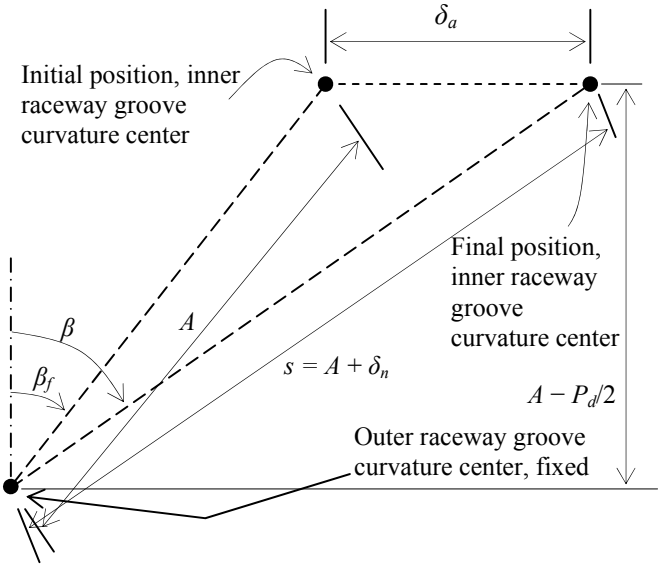

Fig. 7 Positions of ball center and raceway groove curvature centers at angular position ψ, with and without applied load

From Fig. 7 and (19) it can be determined that s, the distance between the curvature centers of the inner and outer ring raceway grooves at any rolling element position ψ, is given by

$$s = A + \delta_n = A\frac{\cos\beta_f}{\cos\beta}. \tag{20}$$

From (18) and (20) yields

$$\delta_a - A\frac{\sin(\beta - \beta_f)}{\cos\beta} = 0. \quad (21)$$

From (16) and (19) yields

$$Q = K_n A^{3/2}\left(\frac{\cos\beta_f}{\cos\beta} - 1\right)^{3/2}. \quad (22)$$

If the external thrust load, F_a, is applied at the bearing's axis of rotation then, for static equilibrium to exist

$$F_a = QZ\sin\beta. \quad (23)$$

Substitution of (22) into (23) yields

$$F_a - ZA^{3/2}K_n\sin\beta\left(\frac{\cos\beta_f}{\cos\beta} - 1\right)^{3/2} = 0. \quad (24)$$

Equation (24) is a nonlinear equation with unknown β. Since K_n is a function of final contact angle, β, the equation must be solved iteratively to yield an exact solution for β.

Taking K_n as a constant (24) may be solved numerically by the Newton-Raphson method. The equation to be satisfied iteratively is well know [5]

$$\beta' = \beta + \frac{\frac{F_a}{ZA^{3/2}K_n} - \sin\beta\left(\frac{\cos\beta_f}{\cos\beta} - 1\right)^{3/2}}{\cos\beta\left(\frac{\cos\beta_f}{\cos\beta} - 1\right)^{3/2} + \frac{3}{2}\tan^2\beta\left(\frac{\cos\beta_f}{\cos\beta} - 1\right)^{1/2}\cos\beta_f}. \quad (25)$$

Equation (25) is satisfied when $\beta' - \beta$ is essentially zero. For each new value β, a new value K_n must be obtained, until there is no measurable difference in the K_n value. This can be achieved through an outer loop where the goal is to do the difference $\beta'' - \beta$ vanish, where β'', as well as β', is an auxiliary variable.

VI. Numerical Results

The Newton-Rhapson method was chosen to solve the nonlinear equation (24). Chosen the rolling bearing, as input must be given the geometric parameters: d_i, d_o, D, Z, r_i and r_o, in accordance with the Figs. 2 and 4, and the elastic properties E_a, E_b, υ_a and υ_b. Next, the following parameters must be obtained: f_i, f_o, B, A, E', d_e, P_d and β_f.

The interest here is to observe the behavior of an angular-contact ball bearing under a known thrust load, which is to be applied statically to the geometric bearing centerline. Let F_a ranges from zero up to the last valid value in Newtons.

Initially the values for β, β' and β'' were adopted as being equal β_f. Then, for each new value of F_a ranging from zero, do $\beta = f_s\beta$, where f_s is the *shock factor*. While the outer loop difference $\beta'' - \beta$ is greater than a minimal error, do $\beta'' = \beta$ and calculate the values: $1/R|_i$, $1/R|_o$, Γ_i, Γ_o, k_i, k_o, $\mathbf{K}_i$, $\mathbf{K}_o$, $\mathbf{E}_i$, $\mathbf{E}_o$, K_i, K_o and K_n in according to previous sections. Do $\beta = f_s\beta$. If the difference $\beta'' - \beta$ is lesser than the minimal error, a new thrust load value is acquired and the procedure is repeated up to the last valid thrust load value, when the program ends.

For each iteration in the outer loop a new value for β' is obtained in the inner loop. The new β' value is compared with the old β and if the difference $\beta' - \beta$ is greater than a minimal error a new iteration in the inner loop occurs. If the difference $\beta' - \beta$ is lesser than the minimal error, the inner loop ends.

To show an application of the theory developed in this work a numerical example is presented here. It was chosen the 218 angular-contact ball bearing, which was also used by Harris [5]. Thus, the results generated here can be compared to a certain degree with the Harris results. The input data for this rolling bearing were the following:

Inner raceway diameter, $d_i = 0.10279$ m
Outer raceway diameter, $d_o = 0.14773$ m
Ball diameter, $D = 0.02223$ m
Ball number, $Z = 16$
Inner groove radius, $r_i = 0.01163$ m
Outer groove radius, $r_o = 0.01163$ m
Modulus of elasticity for both balls and races, $E = 2.075 \times 10^{11}$ N/m^2
Poisson's ratio for both balls and races, $\upsilon = 0.3$

The remaining parameters has been calculated, yielding

Inner race conformity, $f_i = 0.523166891587944$
Outer race conformity, $f_o = 0.523166891587944$
Total conformity ratio, $B = 0.046333783175888$
Initial curvature centers distance, $A = 0.00103$ m
Effective elastic modulus, $E' = 228021978021.978$ N/m^2
Bearing pitch diameter, $d_e = 0.12526$ m
Diametral clearance, $P_d = 0.00048$ m
Free-contact angle, $\beta_f = 39.915616407992260^o$

The initial estimates were the following:

Contact angle, $\beta = \beta' = \beta'' = \beta_f$.

Since it is the qualitative behavior of solutions that is the interest, the results are presented here in graphical form.

The Fig. 8 shows the normal ball load, Q, as a function of the external thrust load, F_a. For a 17,800 N external thrust load Harris found the magnitude of 1,676 N for all balls (p. 249). This work found the magnitude of 1,681.663561507027 N for all balls for the same external thrust load. Assuming correct the results of this work, this means that Harris made an error of about –0.34% in the normal ball load determination.

The Fig. 9 shows the contact angle, β, as a function of the external thrust load, F_a. While Harris has been found a contact angle magnitude of 41.6° for all balls and for a 17,800 N external thrust load (p. 249), this work found the magnitude of 41.417986227161386° for all balls for the same external thrust load. This represents an error of about 0.44% in the contact angle determination.

The Fig. 10 shows the relative axial displacement between inner and outer ring raceways, δ_a, as a function of the external thrust load, F_a. While Harris has been found an axial displacement magnitude of 0.0386 mm (p. 249), this work found the magnitude of 0.0360110954004549 mm for the same external thrust load. This represents an error of about 7.19% in the relative axial displacement determination.

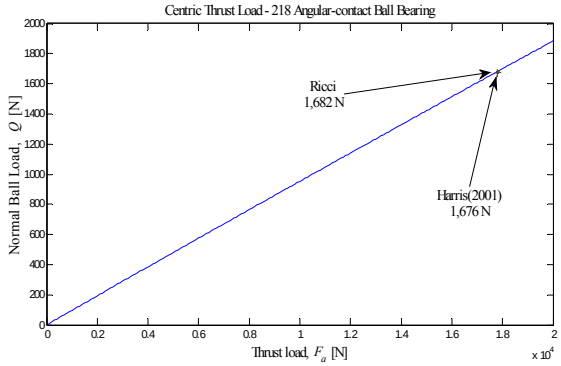

Fig. 8 Normal ball load, Q, as a function of the thrust load, F_a.

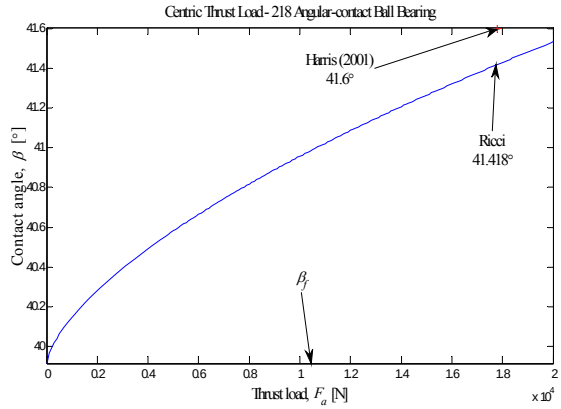

Fig. 9 Contact angle, β, as a function of the thrust load, F_a

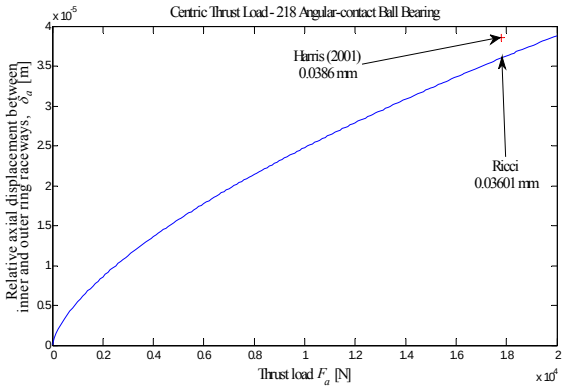

Fig. 10 Axial deflection, δ_a, as a function of the external thrust load, F_a

The Figs. 11 and 12 show the distance between curvature centers, s, and the total ball deflection, δ_n, as functions of the external thrust load, F_a, respectively. The total normal ball deflection can be obtained by summing the maximum normal elastic compressions on the inner and outer races, δ_i and δ_o, or by subtracting A from s, once $\delta_n = s - A$.

The Figs. 13 and 14 show the behavior of the contact angle β and the outer loop auxiliary variable β" during the outer loop numerical procedure. The shock factor adopted was 1.001 and every level, shown in detail, represents a constant value of the external thrust load. The procedure demanded 814 outer loop iterations to cover the range from zero to 20,000 N for the external thrust load, with steps of 100 N. The Figs. 15 and 16 show the behavior of the difference between the outer loop auxiliary variable β" and the contact angle β.

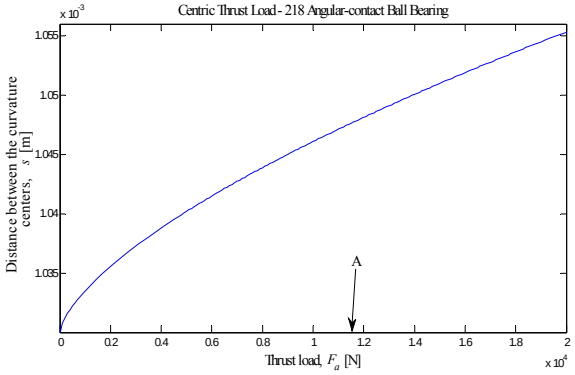

Fig. 11 Distance between curvature centers, s, as a function of the external thrust load, F_a

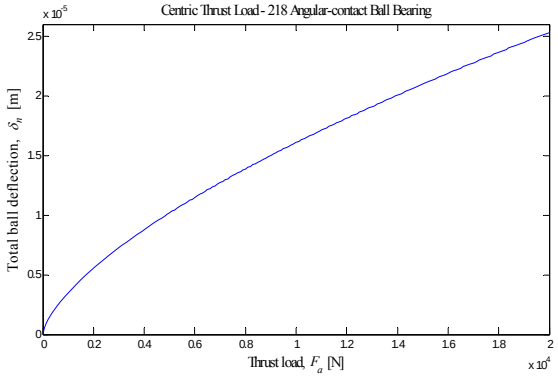

Fig. 12 Total ball deflection, δ_n, as a function of the external thrust load, F_a

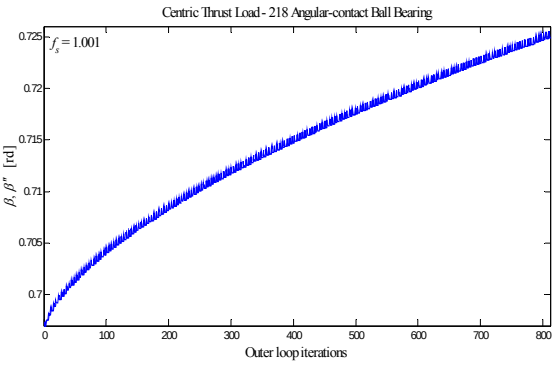

Fig. 13 Convergence procedure of the contact angle β and the outer loop auxiliary variable β"

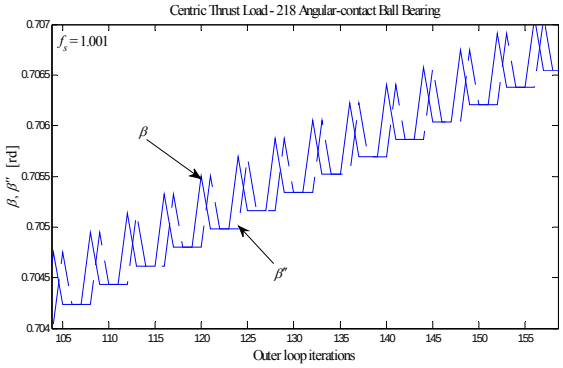

Fig. 14 Convergence procedure of the contact angle β and the outer loop auxiliary variable β'' (detail)

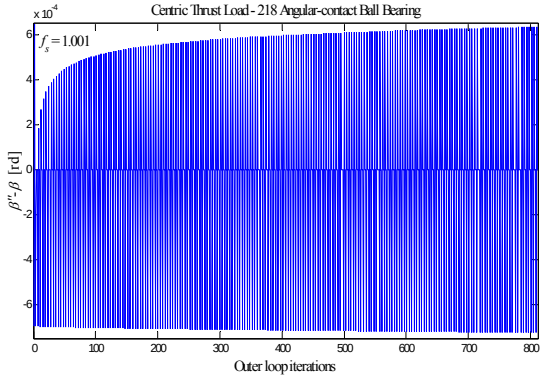

Fig. 15 Convergence procedure of the difference between the outer loop auxiliary variable β'' and the contact angle β

Fig. 16 Convergence procedure of the difference between the outer loop auxiliary variable β'' and the contact angle β (detail)

The Figs. 17 and 18 show the behavior of the contact angle β and the inner loop auxiliary variable β' during the inner loop numerical procedure. The shock factor adopted was 1.001 and every level, shown in detail, represents a constant value of the external thrust load. The procedure demanded 3,879 inner loop iterations to cover the range from zero to 20,000 N for the external thrust load, with steps of 100 N. The Figs. 19 and 20 show the behavior of the difference between the inner loop auxiliary variable β' and the contact angle β.

VII. Conclusion

A known iterative computational procedure was used to internal normal ball loads calculation in statically loaded single-row, angular-contact ball bearings, subjected to a known thrust load which is applied in the inner ring at the geometric bearing center line. Aspects of the numerical procedure and the behavior of the convergence variables were discussed. Results for a 218 angular-contact ball bearing were compared with literature data. Precise applications, as for example, space applications, require a precise determination of the static loading. Models available in literature are approximate and often are not compatible with the desired degree of accuracy. This work can be extended to determine the loading on high-speed bearings where centrifugal and gyroscopic forces do not be discarded. The results of this work can be used in the accurate determination of the friction torque of the ball bearings, under any operating condition of temperature and speed.

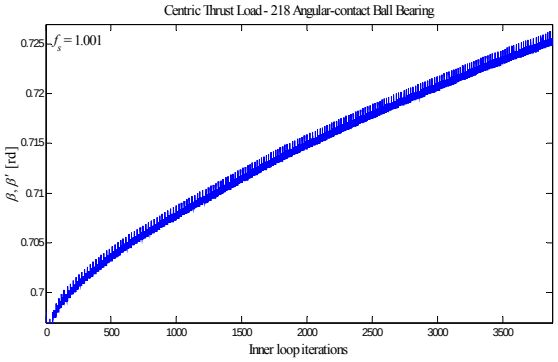

Fig. 17 Convergence procedure of the contact angle β and the inner loop auxiliary variable β'

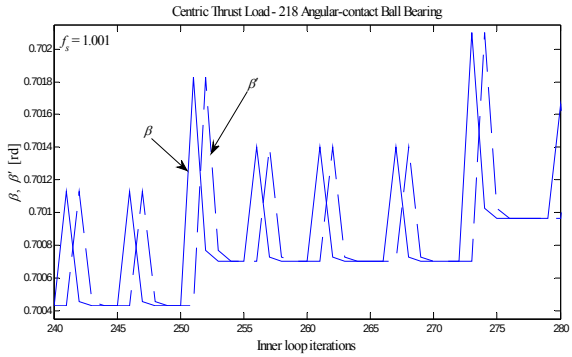

Fig. 18 Convergence procedure of the contact angle β and the inner loop auxiliary variable β' (detail)

References

[1] Stribeck, R. "Ball Bearings for Various Loads," *Trans. ASME* 29, 420-463, 1907.
[2] Sjoväll, H. "The Load Distribution within Ball and Roller Bearings under Given External Radial and Axial Load," *Teknisk Tidskrift,* Mek., h.9, 1933.
[3] Jones, A. *Analysis of Stresses and Deflections,* New Departure Engineering Data, Bristol, Conn., 1946.
[4] Rumbarger, J. "Thrust Bearings with Eccentric Loads," *Mach. Des.,* Feb. 15, 1962.

[5] Harris, T. Rolling Bearing Analysis, 4th ed., John Wiley & Sons Inc., New York, 2001.
[6] Ricci, M. C. *Ball bearings subjected to a variable eccentric thrust load*, DINCON'09 Proceedings of the 8th Brazilian Conference on Dynamics, Control and Applications, May, 18-22, Bauru, Brazil, 2009. ISBN: 978-85-86883-45-3.
[7] Ricci, M. C. *Internal loading distribution in statically loaded ball bearings,* ICCCM09 1st International Conference on Computational Contact Mechanics, Program and Abstracts, p. 21-22, Sept. 16-18, Lecce, Italy, 2009.
[8] Ricci, M. C. *Internal loading distribution in statically loaded ball bearings subjected to a combined radial and thrust load, including the effects of temperature and fit*, Proceedings of World Academy of Science, Engineering and Technology, Volume 57, September 2009, WCSET 2009, Amsterdam, Sept. 23-25, 2009. ISSN: 2070-3724. http://www.waset.org/proceedings.php.
[9] Ricci, M. C. *Internal loading distribution in statically loaded ball bearings subjected to a combined radial and thrust load*, 6th ICCSM Proceedings of the 6th International Congress of Croatian Society of Mechanics, Sept. 30 to Oct. 2, Dubrovnik, Croatia, 2009. ISBN 978-953-7539-11-5.
[10] Ricci, M. C. *Internal loading distribution in statically loaded ball bearings subjected to a combined radial, thrust, and moment load*, Proceedings of the 60th International Astronautical Congress, October, 12-16, Daejeon, South Korea, 2009. ISSN 1995-6258.
[11] Ricci, M. C. *Internal loading distribution in statically loaded ball bearings subjected to an eccentric thrust load*, Submitted to *Mathematical Problems in Engineering*, 2009.
[12] Ricci, M. C. *Internal loading distribution in statically loaded ball bearings subjected to a combined radial, thrust, and moment load, including the effects of temperature and fit*, to be presented at 11th Pan-American Congress of Applied Mechanics, January, 04-10, Foz do Iguaçu, Brazil, 2010.
[13] Hamrock, B. J. and Anderson, W. J. Arched-Outer-Race Ball-Bearing Considering Centrifugal Forces. NASA TN D-6765, 1972.
[14] Hertz, H. "On the Contact of Rigid Elastic Solids and on Hardness," in *Miscellaneous Papers*, MacMillan, London. 163-183, 1896.
[15] Hamrock, B. J. and Anderson, W. J. Rolling-Element Bearings. NASA RP 1105, 1983.

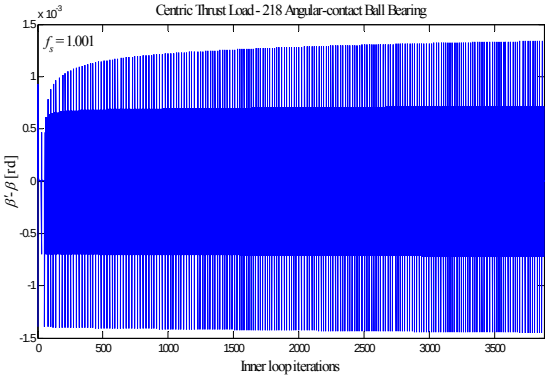

Fig. 19 Convergence procedure of the difference between the inner loop auxiliary variable β' and the contact angle β

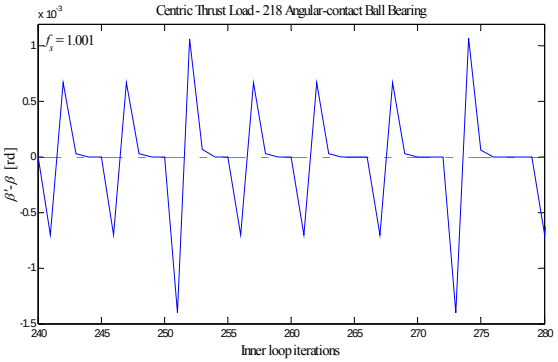

Fig. 20 Convergence procedure of the difference between the inner loop auxiliary variable β' and the contact angle β (detail)